Low Losses Left Handed Gammadion–Fishnet Chiral Metamaterials

O. Fernández, Á. Gómez, A. Vegas, G. J. Molina-Cuberos, A. J. García-Collado

***Abstract*—Negative refraction has many potential applications in the Information and Communications Technology field. However, the high losses of most negative refraction materials prevents the use of this novel property in the implementation of practical devices in the HF range. In attempt to overcome this inconvenience, we present two Gammadion-Fishnet chiral metamaterial structures, constituted by the combination of a lossy chiral metamaterial and different fishnet structures. The electromagnetic characterization of the proposed metamaterials provides a larger bandwidth with negative refraction as well as lower losses when is compared with the initial structures. The results were obtained by using both numerical and experimental data which supports our designs.**

***Index Terms*—chiral; fishnet; metamaterial; low losses; refractive index.**

I. Introduction

ELECTROMAGNETIC metamaterials (MM) are sub-wavelength artificial periodic structures engineered to produce effects not present in natural media, such as negative refraction. Negative index metamaterials (NIM), originally proposed by [1] present simultaneously negative permittivity (ε_r) and permeability (μ_r). Since the first NIM structure was manufactured [2], other bi-layered structures like cut-wire pairs [3] or fishnet structures [4] have been published. However, the need for simultaneous negative ε_r and μ_r is a handicap, especially at high frequencies where negative permeability is more difficult to obtain.

Chiral Metamaterials (CMM) provide an alternative route to negative refraction [5], [6] with no need for simultaneous negative ε_r and μ_r. Chiral media modelling uses the chirality parameter, κ, to quantify the coupling between electric and magnetic fields. If κ is large enough, so that $|\Re(\kappa)| > \left|\Re\left(\sqrt{\varepsilon_r \mu_r}\right)\right|$, the refractive index of the right- (+, RHCP) or left-handed (−, LHCP) circularly polarized (CP) eigenwaves, $n_\pm = \sqrt{\varepsilon_r \mu_r} \pm \kappa$, becomes negative.

High losses in the frequency band with negative refraction is a common drawback of MMs and CMMs. The Figure of Merit, FoM, defined as the ratio between the real and imaginary part of the refractive index n, is a commonly used parameter to quantify the losses [7]. Most of the CMM structures presented in the literature, such as [8]-[12], report FoM values lower than 10.

Different alternatives for minimizing losses in NIM have been proposed such us optimizing the geometry [13], using fishnet structures [14] or using composite CMMs [15].

In this paper, we propose a way to reduce the losses of a chiral metamaterial structure (the conjugated gammadion [10]) by adding to the CMM low losses fishnet arrangements [4], [14]. Unlike the structure proposed in [15], where the negative refraction bandwidth is shifted away from the lossy frequency band region, this paper focuses on reducing the loss region itself.

As a first step, in previous communications [16], [17] two CMM structures were introduced, both showing promising results for reducing losses in the negative refraction region. The analysis of this type of gammadion-fishnet chiral structures is taken one step further by a more detailed study of these new designs and a qualitative explanation of the loss reduction mechanism. To support the numerical study, samples of two structures have been manufactured and experimentally characterized. Both numerical simulations and experiments data show how the addition of fishnet structures to a conjugated gammadion enlarges the negative refraction bandwidth and decreases the losses compared with the initial structure.

II. Gammadion–Fishnet Chiral Metamaterials

A. Geometrical Models

The CMM structures proposed in this paper merge the conjugated gammadion (CG), originally studied by Zhao *et al.*, [10], with two different fishnet metallic patterns. The first is composed by two orthogonal continuous metallic strips that intersect in the center of each face of the unit cell (Fig. 1b), and the second one adds to the previous crossed strips a metallic square patch centered in the unit cell (Fig. 1c), forming an isotropic-like fishnet [4].

Manuscript received May 17, 2019; revised Jul 24, 2019; accepted for publication Aug 18, 2019.

This work has been partially supported by the Spanish Government MINECO through the ERDF co-funded Research Projects TEC2014-55463-C3-1-P and TEC2014-55463-C3-3-P, PGC2018-098350-B-C21 and PGC2018-098350-B-C22.

O. Fernández, Á. Gómez and A. Vegas are with the Departamento de Ingeniería de Comunicaciones, University of Cantabria, Santander, Spain (e-mail: fernanos@unican.es, gomezal@unican.es, vegasa@unican.es).

G. J. Molina-Cuberos is with the Departamento de Electromagnetismo y Electrónica, University of Murcia, Murcia, Spain (e-mail: gregomc@um.es).

A. J. García-Collado is with the Departamento de Geomática, Teledetección y SIG Aplicados, Catholic University of Murcia, Murcia, Spain (e-mail: ajgarcia@ucam.edu).

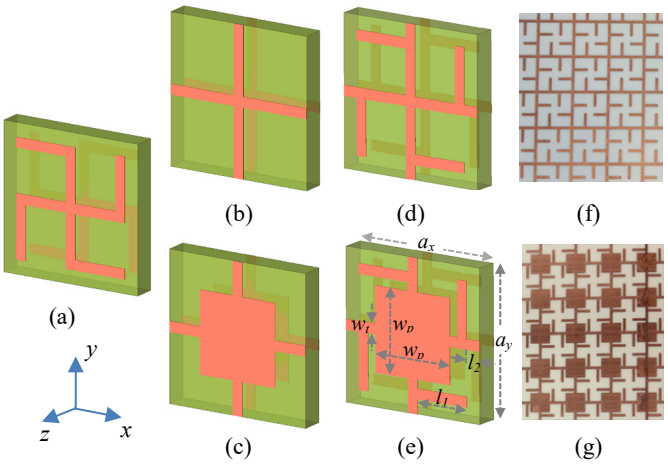

Fig. 1. (a) Conjugated gammadion (b) Fishnet, (c) Modified Fishnet, (d) FCMM, (e) PFCMM and manufactured samples of the FCMM (f) and PFCMM (g) structures.

Combining the CG with each of the fishnet arrangements, the Fishnet Chiral Metamaterial (FCMM), Fig. 1d, and the Patched FCMM (PFCMM) structures, Fig. 1e, are obtained. In order to compare the electromagnetic response of both structures, the same geometrical dimensions were chosen: l_1 = 3.7 mm, l_2 = 0.95 mm, w_t = 0.7 mm and $a_x = a_y$ = 10 mm. The size of the square patch of the PFCMM, w_p = 5.5 mm, is obtained by an optimization process which minimizes losses with respect to the FCMM and maximizes the bandwidth with negative refractive index. Both structures present C_4 symmetry, the FCMM pattern being a limit case of the PFCMM one when $w_p = w_t$. The samples were built on Rogers RO4003C substrate with ε_r = 3.55, $tan\ \delta$ = 0.0027, thickness d = 1.52 mm and a copper cladding of 35 µm.

B. Numerical and Experimental Characterization

The samples have been characterized by using a standard parameter retrieval algorithm for chiral metamaterials [18]. The characterization method assumes linearly polarized incident waves, normal incidence and requires the determination of the co-polar and cross-polar transmission coefficients, t_{Co} and t_{Cross} and co-polar reflection coefficients, r_{Co}. The transmission ($t_{\pm\pm} = t_{Co} \mp j \cdot t_{Cros}$) and reflection ($r$=$r_{Co}$) coefficients for RHCP and LHCP are obtained by making use of the Jones Matrix notation [19]. The first sub-index in t_{++} represents the handedness of the transmitted wave, while the second one represents the handedness of the incident wave. The reflection coefficient r is equal for both handedness since the impedance is the same for RH- and LHCP.

The normalized impedance (Z) and the refractive indices for the RHCP (n_+) and LHCP (n_-) waves are obtained from

$$Z = \pm\sqrt{\frac{(1+r)^2 - t_{++}t_{--}}{(1-r)^2 - t_{++}t_{--}}} \tag{1}$$

$$n_{\pm} = \frac{1}{k_0 d}\left\{-angle\left(\frac{1}{t_{\pm\pm}}\left(1-\frac{Z-1}{Z+1}r\right)\right) + 2m\pi + j\cdot\ln\left|\frac{1}{t_{\pm\pm}}\left(1-\frac{Z-1}{Z+1}r\right)\right|\right\} \tag{2}$$

with m=0,1,2,.. The sign in (1) is chosen according to the energy conservation principle for a passive material (for an $e^{j\omega t}$ time-harmonic convention $\Re(Z) > 0$ and $\Im(n_{\pm}) < 0$, with $\Re(\cdot)$ and $\Im(\cdot)$ representing the real and imaginary parts respectively of a complex number). The branch of m in (2) can be determined by assuming that the refraction index is similar to the background material and by applying continuity conditions far from the resonances.

From Z and $n_{\pm}$, the equivalent characteristic parameters are obtained as follows:

$$n = \frac{n_+ + n_-}{2};\quad \kappa = \frac{n_+ - n_-}{2};\quad \varepsilon = \frac{n}{Z};\quad \mu = nZ \tag{3}$$

The transmission and reflection coefficients for linearly polarized incident waves were obtained through numerical simulations and experiments. The numerical analysis was carried out through full wave electromagnetic simulations using the Finite Differences Time Domain technique in Keysight EMPro 3D EM simulation software. For this purpose, a single unit cell is considered with periodic boundary conditions in the x and y directions and perfect absorbing layers in the z direction. For the experimental characterization, samples with 22 x 22 unit cells, Fig. 1f and 1g, were manufactured by chemical etching. The measurements were obtained using an Agilent E8362A PNA Series Network Analyzer, and two standard gain horn antennas. The sample holder consists of a wood sheet covered by absorbent material with a square 19 cm wide opening in its center to place the sample. We have performed several measurements to determine the optimum separation between the antennas and the sample holder in order to maximize the field coupled on the metamaterial, reduce multiple reflections between sample and antennas and minimize the spurious propagation paths between antennas. The best results were obtained for separations of approximately 1 m.

III. RESULTS AND DISCUSSION

A. Fishnet Chiral Metamaterial

Fig. 2 shows the transmission and reflection coefficients obtained from simulations for the CG (2a) and from simulations and measurements for the FCMM (2b). The good agreement reached between measurements and simulations for the FCMM case confirms the simulation model. A comparison of both figures shows that their frequency responses are quite similar in shape although with a frequency shift of about 4.5 GHz. Both plots present a high cross-polar transmission peak that coincides in frequency with a deep reflection dip. These similarities are due to the fact that both structures are formed by the same particles, the conjugated omegas (CO) particle, Fig. 3a, although arranged in a different way. A couple of orthogonal and overlapped CO forms the CG structure [10], Fig. 3b. For the FCMM structure, the fishnet wires produce new electric connections among unit cells that generates new pairs of non-overlapped horizontal and vertical resonant CO structures, identified in Fig. 3c as CO_{Hn} and CO_{Vn} respectively. The smaller size of these new CO particles provides an upward frequency shift, which can be tuned by modifying the cell size; changing a_x modifies the segments defined in Fig. 1 as l_2, and thus varies the central segment of the CO_{Hn} and CO_{Vn} structures.

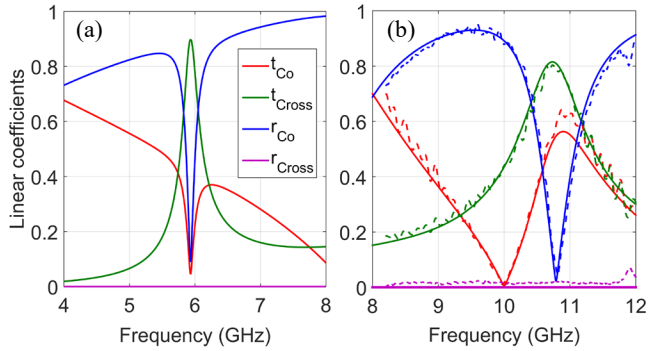

Fig. 2. Transmission and reflection coefficients of the (a) CG (simulations) and (b) the FCMM (simulations and measurements). Solid line – Simulations, Dash line – Measurements.

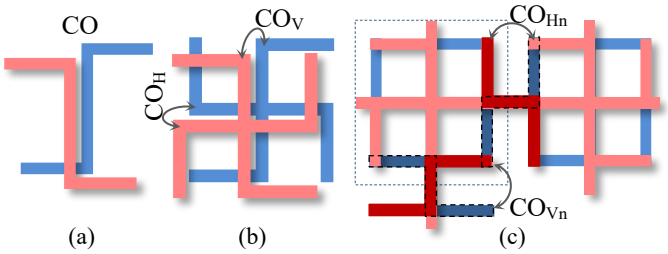

Fig. 3. (a) Conjugated Omega (CO) particle. Combination of CO particles in (b) the CG and in (c) the FCMM structure. The red colour represents the top layer and the blue colour the bottom one. COv (CO_H) represents a CO with its central segment vertically (horizontally) aligned. The new CO structures formed in (c) by the addition of the fishnet, CO_{Vn} and CO_{Hn}, are highlighted with a darker colour.

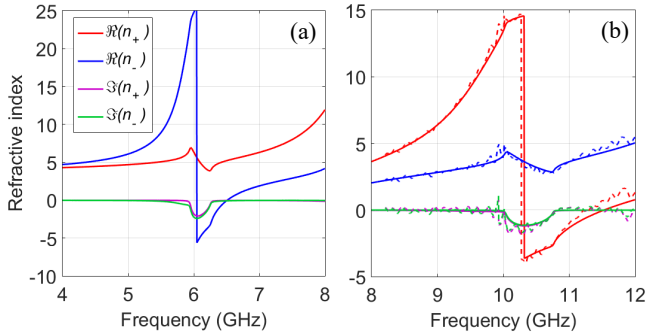

Fig. 4. Refractive indices $n_{\pm}$ of the CG (a) and the FCMM (b). Solid line – Simulations, Dash line – Measurements.

Fig. 4 presents the refractive indices n_+ and n_- of both structures. We can observe that their responses are interchanged. For the gammadion case, the LHCP eigenmode resonates and presents negative refraction, Fig. 4a, while for the FCMM case the resonance appears in the RHCP eigenmode. This change is due to the opposite handedness of CO_H and CO_V, see Fig. 3b, compared with CO_{Hn} and CO_{Vn}, Fig. 3c.

Just above the resonance frequency, the refractive indices present negative values. Near the resonances the losses, i.e. $|\Im(n_{\pm})|$, are relatively high. However, there is a short bandwidth (BW) in both structures where $\Re(n_{\pm})$ is still negative and $\Im(n_{\pm})$ tends to zero, i.e. low losses. Comparing both responses, we can observe that the FCMM presents a BW of 0.75 GHz that is around 13 times larger than the CG bandwidth. The negative refractive indices in both cases present typical values for such materials, in the range between -2 and 0. However, due to the strong reduction of the imaginary part, the FoM(n_+) of the FCMM case reaches a maximum of 38, whereas the highest FoM(n_-) for the CG case is only 10.

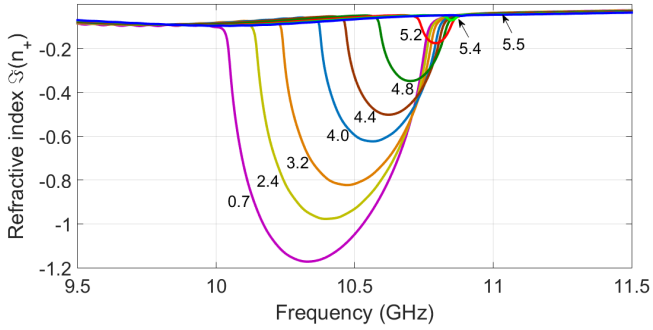

Fig. 5. Imaginary component of n_+ for different values of patch side (w_p).

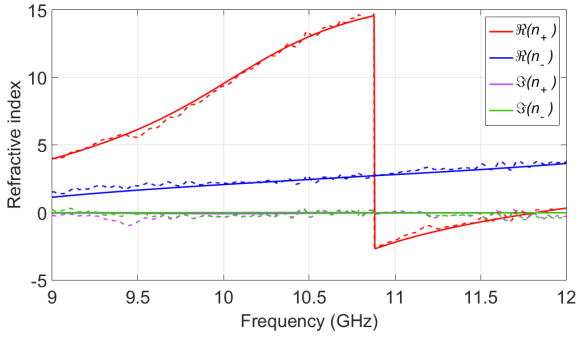

Fig. 6. Refractive indices $n_{\pm}$ of the PFCMM. Solid line – Simulations, Dash line – Measurements.

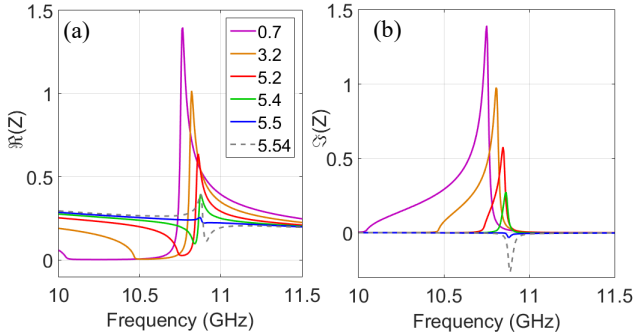

Fig. 7. Normalized wave impedance as a function of w_p, (a) $\Re(Z)$, (b) $\Im(Z)$

B. *Patched Fishnet Chiral Metamaterial*

The PFCMM structure is an improved variation of the FCMM that includes a square patch to reduce losses. The most suitable patch side length, w_p, was obtained through an optimization process. Fig. 5 shows $\Im(n_+)$ for several values of w_p. It can be clearly seen that the longer the patch side is the lower the losses are, getting the optimum case for $w_p = 5.5$ mm.

Fig. 6 shows the refractive indices of optimized PFCMM structure obtained by simulations and measurements. A notable increase of up to 20% of BW compared with the FCMM case and 15 times larger than the BW of CG can be observed. Furthermore, FoM(n_+) reaches a maximum value of 56, which is almost 50% higher than the FCMM case.

The losses reduction in the frequency region with negative refraction can be better understood by looking into the normalized wave impedance of the PFCMM. Fig. 7 shows the real and imaginary parts of Z as a function of the patch size. The non-patched structure (FCMM case), with w_p = 0.7 mm, mainly

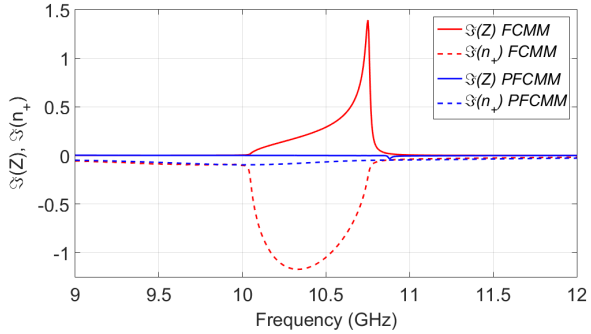

Fig. 8. Imaginary parts of Z and n_+ for the FCMM and PFCMM structures.

presents an inductive behavior, $\Im(Z) > 0$, due to the metallic wires of the fishnet grid. As the size of the patch increases, the inductive effect of the wires is partially compensated by the capacitance of the parallel-plate capacitor formed by the two metallic patches. Therefore, Z is less dispersive, $\Re(Z)$ converges to a straight line with values between 0.2 and 0.3 and $\Im(Z)$ tends to zero. When w_p = 5.5 mm, the inductive and capacitive effects are counterbalanced and therefore $\Im(Z)$ is close to zero. For bigger patch sides, the capacitive effect is predominant and thus $\Im(Z)$ becomes negative and the material more dispersive.

The variation of the reactance produced by changing the patch size has a direct effect over the chiral metamaterial losses. From Fig. 5 and Fig. 7b we can observe that both $\Im(n_+)$ and $\Im(Z)$ tend to 0 as w_p tends to 5.5mm. Fig. 8 represents the reactance and $\Im(n_+)$ for two limit cases. The first case, red lines, represents a structure without patch (FCMM). In this situation, in the frequency band where $\Im(Z) \neq 0$ the structure presents a lossy behavior with $\Im(n_+) \neq 0$. With the optimum patch size, blue lines, the reactance is null and $\Im(n_+)$ is also very close to zero. In these conditions the proposed structure presents negative refraction but with low loss.

IV. Conclusion

In this work, two new low loss chiral metamaterial structures constituted by merging a lossy chiral metamaterial, a conjugated gammadion, with two fishnet structures are presented. These proposed structures were modeled and characterized by using numerical simulations and experiments and a very good agreement was found.

These structures show a great improvement in the FoM of the refractive indices and the bandwidth with negative refraction index compared with the starting structure, the conjugated gammadion. In the case of the FCMM, the FoM(n_+) increases almost by a factor of four, up to 38, while the bandwidth with negative refraction enlarges by a factor of 13, up to 0.77 GHz. The FCMM is optimized with the inclusion of a metallic patch that counterbalances the inductive response of the wires of the fishnet. Consequently, losses decrease, FoM increases and the negative refraction bandwidth is enlarged. The optimized patched structure presents a FoM(n_+) = 56 and a bandwidth of 0.9 GHz with negative refraction index. The properties of the designed structures make them suitable candidate for applications requiring negative refraction.

Acknowledgment

The authors thank the company 2CISA for implementing the structures and M. López, from the University of Cantabria, for his useful work in the sample holder implementation.

References

[1] V. G. Veselago, "The electrodynamics of substances with simultaneously negative values of ε and μ," *Sov. Phys. Usp.* 10 pp. 509–514, 1968.

[2] D. R. Smith, W. J. Padilla, D. C. Vier, S. C. Nemat-Nasser and S. Schultz, "A composite medium with simultaneously negative permeability and permittivity," *Phys. Rev. Lett.* 84, pp. 4184–7, 2000.

[3] K. Guven, M.D. Caliskan, and E. Ozbay, "Experimental observation of left-handed transmission in bilayer metamaterial under normal-to-plane propagation," *Opt. Express,* vol. 4, pp. 8685-8693, 2006.

[4] M. Kafesaki, I. Tsiapa, N. Katsarakis, Th. Koschny, C. M. Soukoulis, and E. N. Economou, "Left-handed metamaterials: The fishnet structure and its variations," *Phys. Rev. B*, vol. 75, 235114, 2007.

[5] S. Tretyakov, I. Nefedov, A. Sihvola, S. Maslovski and C. Simovski, "Waves and energy in chiral nihility," *J. Electromagn. Waves Appl. vol.* 17 pp. 695–706, 2003.

[6] J. B. Pendry, "A chiral route to negative refraction," *Science*, vol. 306, no. 5700, pp. 1353–1355, 2004.

[7] C. M. Soukoulis and M. Wegener, "Past achievements and future challenges in the development of three-dimensional photonic metamaterials," *Nature Photonics,* vol. 5, pp. 523–530, 2011.

[8] E. Plum, J. Zhou, J. Dong, V. A. Fedotov, T. Koschny, C. M. Soukoulis, and N. I. Zheludev, "Metamaterial with negative index due to chirality," *Phys. Rev. B*, vol. 79, 035407, Jan 2009.

[9] D. Zarifi, M. Soleimani and V. Nayyeri, "Dual- and Multiband Chiral Metamaterial Structures With Strong Optical Activity and Negative Refraction Index," *IEEE Antennas Wireless Propag. Lett.*, vol. 11, pp. 334-337, 2012.

[10] R. Zhao, L. Zhang, J. Zhou, Th. Koschny, and C. M. Soukoulis, "Conjugated gammadion chiral metamaterial with uniaxial optical activity and negative refractive index," *Phys. Rev. B*, vol. 83, 35105, 2011.

[11] J. Li, F.-Q. Yang, and J.-F. Dong, "Design and simulation of L-shaped chiral negative refractive index structure," *Prog. Electromagn. Res.*, vol. 116, pp. 395–408, 2011.

[12] D. Zarifi, M. Soleimani, V. Nayyeri and J. Rashed-Mohassel, "On the Miniaturization of Semiplanar Chiral Metamaterial Structures," *IEEE Trans. Antennas Propag.*, vol. 60, no. 12, pp. 5768-5776, Dec. 2012.

[13] D.Ö. Güney, T. Koschny, and C.M. Soukoulis, "Reducing ohmic losses in metamaterials by geometric tailoring," *Phys Rev B,* vol. 80, 2009.

[14] J. Zhou, T. Koschny, and C. M. Soukoulis, "An efficient way to reduce losses of left-handed metamaterials," *Opt. Express*, vol. 16, pp. 11147–11152, 2008.

[15] Z. F. Li, K. B. Alici, H. Caglayan, M. Kafesaki, C. M. Soukoulis, and E. Ozbay, "Composite chiral metamaterials with negative refractive index and high values of the figure of merit," *Opt. Express*, vol. 20, pp. 6146–6156, 2012.

[16] O. Fernández, Á. Gómez, A. Vegas, G. J. Molina-Cuberos, and A. J. García-Collado, "Losses reduction in composite chiral metamaterials," The 36th PIERS in Prague, Czech Republic, 6-9 July, 2015.

[17] O. Fernández, Á. Gómez, A. Vegas, G. J. Molina-Cuberos and A. J. García-Collado, "Novel fishnet-like chiral metamaterial structure with negative refractive index and low losses," *2017 IEEE International Symposium on Antennas and Propagation & USNC/URSI National Radio Science Meeting*, San Diego, CA, pp. 1959-1960, 2017.

[18] R. Zhao, T. Koschny, and C. M. Soukoulis, "Chiral metamaterials: retrieval of the effective parameters with and without substrate," *Opt. Express*, vol. 18, no. 14, pp. 14553–14567, 2010.

[19] G. J. Molina-Cuberos, Á. J. Garcia-Collado, I. Barba and J. Margineda, "Chiral Metamaterials With Negative Refractive Index Composed by an Eight-Cranks Molecule," *IEEE Antennas Wireless Propag. Lett.*, vol. 10, pp. 1488-1490, 2011.